www.crt-journal.org

Crystal Research and Technology

Journal of Experimental and Industrial Crystallography
Zeitschrift für experimentelle und technische Kristallographie

WILEY-VCH

Cryst. Res. Technol. **48,** No. 3, 153–162 (2013) / **DOI** 10.1002/crat.201200443

The mineral component of human cardiovascular deposits: morphological, structural and crystal-chemical characterization

S. N. Danilchenko*[1], V. N. Kuznetsov[1], A. S. Stanislavov[1], A. N. Kalinkevich[1], V. V. Starikov[2], R. A. Moskalenko[3], T. G. Kalinichenko[1], A. V. Kochenko[1], Jinjun Lü[4], Jian Shang[4], and Shengrong Yang[4]

[1] Institute for Applied physics, NAS of Ukraine, Sumy, Ukraine
[2] National Technical University "Kharkov Polytechnic Institute", Kharkov, Ukraine
[3] Sumy State University, Medical Institute, Sumy, Ukraine
[4] Lanzhou Institute of Chemical Physics, Chinese Academy of Sciences, Lanzhou, P.R.China

Received 28 October 2012, revised 22 February 2013, accepted 25 February 2013
Published online 18 March 2013

Key words bioapatite, nanocrystal, cardiovascular calcification, phase content, crystallinity, morphology.

Complementary experimental techniques were applied to characterize bioapatite nanocrystals from pathological cardiovascular deposits. The investigated collection included the leaflets from aortic valve, leaflets from mitral valve, leaflets from tricuspid valve and calcified aorta's wall. XRD, EDX and FTIR data have shown that all studied samples consist of imperfect apatite with different crystallinity and variable chemical composition. In accordance with TEM data, the crystals of pathological calcified deposits frequently have oblong or rod-like shape (length of 60-90 nanometers, width of 20-30 nanometers). At the same time, in the SEM and TEM experiments, the complex spheroid assemblies and planar sheet-like shaped formations with crystal structure close to apatite were observed. Probably, the different shape and morphology of the particles are caused by different ways of crystal nucleation and growth, although the exact mechanisms remain an open question.

1 Introduction

Pathological deposition of biocrystals is a widespread phenomenon in numerous acute and chronic diseases such as advanced arteriosclerosis, diabetes, chronic renal failure and many others. Worldwide, many elderly persons suffer from the pathology, which is characterized by encrustation of heart valve leaflets with mineral deposits [1–3]. The exact mechanisms underlying these processes remain unclear. Calcified aorta's walls, aortic and mitral heart valve deposits can be considered as the main examples of cardiovascular calcifications.

Several researchers have characterized the mineral component of cardiovascular calcification [4–7] and found that the major calcium phosphate phase is bioapatite (idealized empirical formula $Ca_{10}(PO_4)_6(OH)_2$), similar to that observed in bone. More precisely, mineral component of calcified deposits is represented by nonstoichiometric carbonate-containing imperfect apatites with variable Ca/P atomic ratio and substitutions in anionic and cationic sublattices [1,2,4]. However, the current knowledge about the ectopic bioapatite crystals is not complete, despite of well-defined phase composition and general crystal-chemical characteristics. The microstructure, ultrastructural organization and non-crystalline component (crystals' environment) of ectopic mineral particles can be regarded as insufficiently studied aspects. The early precursors of bioapatite in pathological calcifications are also ambiguous.

The main difficulties in the investigation of pathologically calcified deposits are 1) the presence of water and organic component, 2) low crystallinity with probable phase non-homogeneity and 3) small amount of material, not allowing to apply all experimental techniques. The conditions of sample preparation are also important for correct analysis of ectopic biominerals. Therefore, these issues need to be carefully studied, and the techniques used for examination of pathological biominerals should be developed and improved.

* Corresponding author: e-mail: danil50@hotbox.ru

Table 1 The list of the samples with the chart of examination.

Samples		XRD			IRS	SEM/EDX	TEM/SAED
		RT*	T=200 °C	T=900 °C			
1	Aortic valve 1	+		+	+	REMMA102	–
2	Aortic valve 2	+		+	+	REMMA102	–
3	Aortic valve 3	+		+	+	REMMA102	–
4	Aortic valve 4	+		+	+	REMMA102	–
5	Mitral valve 1		+	+	–	JSM5600 LV	JEM2010
6	Mitral valve 2		+	+	–	REMMA102	–
7	Mitral valve 3		+	+	–	–	–
8	Mitral valve 4		+	+	–	–	–
9	Mitral valve 5		+	+	–	REMMA102	–
10	Calcified aorta's wall 1		+	+	–	–	–
11	Calcified aorta's wall 2		+	+	–	–	–
12	Calcified aorta's wall 3		+	+	–	REMMA102	–
13	Calcified aorta's wall 4**		–	–	–	JSM5600 LV	JEM2010
14	Calcified aorta's wall 5		+	+	–	–	–
15	Tricuspid valve 1	+		+	+	REMMA102	TEM125K
16	Tricuspid valve 2	+		+	–	REMMA102	–
17	Tricuspid valve 3	+		+	–	REMMA102	–

*RT – stands for room temperature. The materials from aortic valves and tricuspid valves were not exposed to thermal treatment before examination by REMMA, TEM and IRS. **The sample number 13 (Calcified aorta's wall 4) was the only sample subjected to SEM and TEM investigation but not to XRD due to the insufficient amount of material for XRD examination.

Numerous studies demonstrate that the structural investigations of biological apatite subjected to the annealing at specific temperatures can give additional valuable information via the analysis of thermal behavior of mineral and phase decomposition products [e.g., 8,9]. The thermogravimetry data can give information about the composition of an ectopic deposit sample: water content, mineral content, and amount of carbonate fraction in the mineral phase [4,6]. Moreover, it allows distinguishing the loosely adsorbed water loss (ca. 200 °C) and bound water elimination (ca. 600 °C), as well as complete organic fraction decomposition. Heating bioapatite above 900 °C causes the thermal decomposition of imperfect apatite with the formation of stoichiometric one, plus tricalcium phosphate (β-TCP, $Ca_3(PO_4)_2$), or magnesium substituted tricalcium phosphate $(Ca,Mg)_3(PO_4)_2$ (β-TCMP), or/and other crystal phases [9–11].

The objective of this work is to perform a comparative analysis of a representative set of human cardiovascular deposits by several instrumental methods with some variations of the sample pretreatment procedure, including heat treatment. In general, this work is aimed to investigate the possibility of gaining supplementary structural and ultrastructural information about bioapatite extracted from pathological cardiovascular deposits using complementary techniques.

2 Materials and methods

Sample Preparation All samples were obtained from two medical institutes where anatomical analysis, histomorphology, histochemistry and medical morphometry of them have been performed. The investigated collection (table 1) includes the leaflets from aortic valves (four cases), leaflets from mitral valves (five cases), leaflets from tricuspid valves (three cases) and calcified aortas' walls (five cases). A part of the mineralized tissue samples (aortic valves and tricuspid valves) was fixed in formalin and dried in air. After that the regions of macroscopic calcification exhibiting small white-brownish grains were carefully separated with the scalpel from non-calcific material. These samples were not exposed to thermal or chemical treatment to prevent any alteration of their initial structure. Other samples (mitral valves and calcified aortas walls) after manual pretreatment (separation, cleaning and drying) were annealed in the electric furnace in air under the temperature of 200 °C during one hour. This guarantees the removal of the non-crystalline water and thermal decomposition of organic component [4,6]. Before examination by each method all samples were powdered in a mortar, excluding the scanning electron

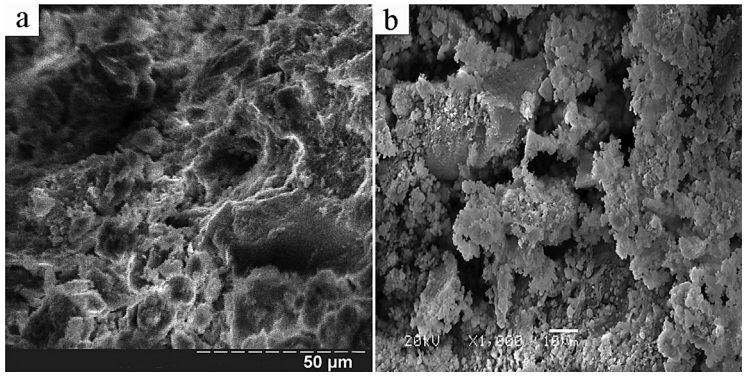

Fig. 1 Typical SEM images of cardiovascular deposits: (a) Aortic valve 2 (magnification 1500, REMMA102; (b) Calcified aorta's wall 4 (magnification 1000, JSM5600LV).

microscopy. In addition, the material of the pathological deposits was subjected to annealing in the electric furnace in the air under the temperature of 900 °C during one hour and characterized again by X-ray diffraction (XRD).

Data acquisition and processing The inorganic materials in the initial state and heated at 200 °C were characterized by scanning electron microscopy (SEM) with X-ray microanalysis using the microscopes JSM5600LV (JEOL, Japan) and REMMA102 (SELMI, Ukraine) coupled with energy-dispersive X-ray (EDX) spectrometer. To avoid the surface charge accumulation in the electron-probe experiment, the samples were covered with a thin (30-50 nm) layer of gold. Quantification of the elemental composition was done using the ZAF routine: atomic number Z, absorption and fluorescence correction [12].

XRD investigations were performed using the diffractometer DRON4-07 ("Burevestnik", Russia) connected to the computer-aided experiment control and data processing system. The Ni-filtered CuKα radiation (wavelength 0.154 nm) was used with a conventional Bragg-Brentano ϑ-2ϑ geometry (2ϑ is the Bragg's angle). The current and the voltage of the X-ray tube were 20 mA and 30 kV respectively. The samples were measured in the continuous registration mode (at the speed of 1.0 °/min) within the 2ϑ-angle range from 10° to 60°. All data processing procedures were carried out with the use of the program package DIFWIN-1 ("Etalon PTC" Ltd, Russia). The separation of overlapping diffraction lines was done with the freeware program New_Profile 3.4 (http://remaxsoft.ru/). Phase analysis was carried out by comparing the diffraction patterns from the investigated samples and the reference data JCPDS.

Infrared spectra (IRS) in the range of 4000−400 cm^{-1} were recorded by the Spectrum-One FTIR spectrometer (Perkin Elmer). Before the measurements the powdered samples were mixed with the KBr powder (2.5-3.0 mg of a sample per 300 mg of KBr) and pressed to tablets.

The morphologies of the deposits' crystals were observed by transmission electron microscopes (TEM) JEM2010 (JEOL, Japan) and TEM125K (SELMI, Ukraine). To obtain isolated crystals before TEM examinations the samples were ultrasonically disaggregated (120 W, 22 kHz output frequency). The selected area electron diffraction pattern (SAED) was performed at accelerated voltage of 200 kV (JEM2010) and 90 kV (TEM125K).

The list of the samples is given in the table 1. Actually, the XRD was the basic method of investigation, while IRS, TEM with SAED, and SEM with EDX analyses were applied not for all samples.

3 Results and discussion

According to the SEM data, the untreated pathological deposits showed a porous or spongy and slightly perforated structure consisting of lamellar microparticles (figure 1a). The samples annealed at 200 °C revealed agglomerates and separated mineral particles in a wide range of shapes and sizes (figure 1b), suggesting the loss of continuity caused by thermal pyrolysis of organic components.

The EDX patterns showed only Ca and P signals in most cases (see figure 2a as an example). However, in a few cases the prominent signals from other elements were clearly seen. The most demonstrative example of that kind was the Calcified aorta's wall 4, showing K, Cl, Fe and S peaks in addition to Ca and P (figure 2b). From

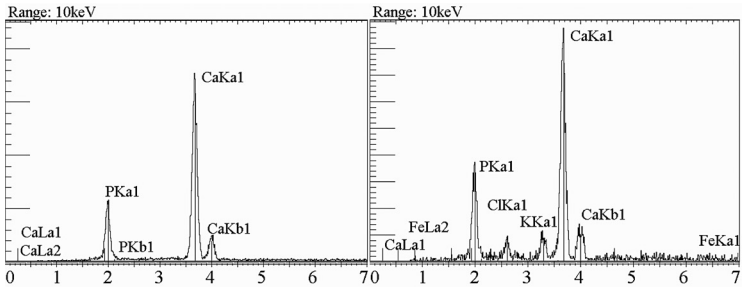

Fig. 2 The EDX patterns of cardiovascular deposits containing only Ca and P peaks (left, sample Mitral valve 1) and containing K, Cl, Fe and S peaks in addition to Ca and P (right, sample Calcified aorta's wall 4).

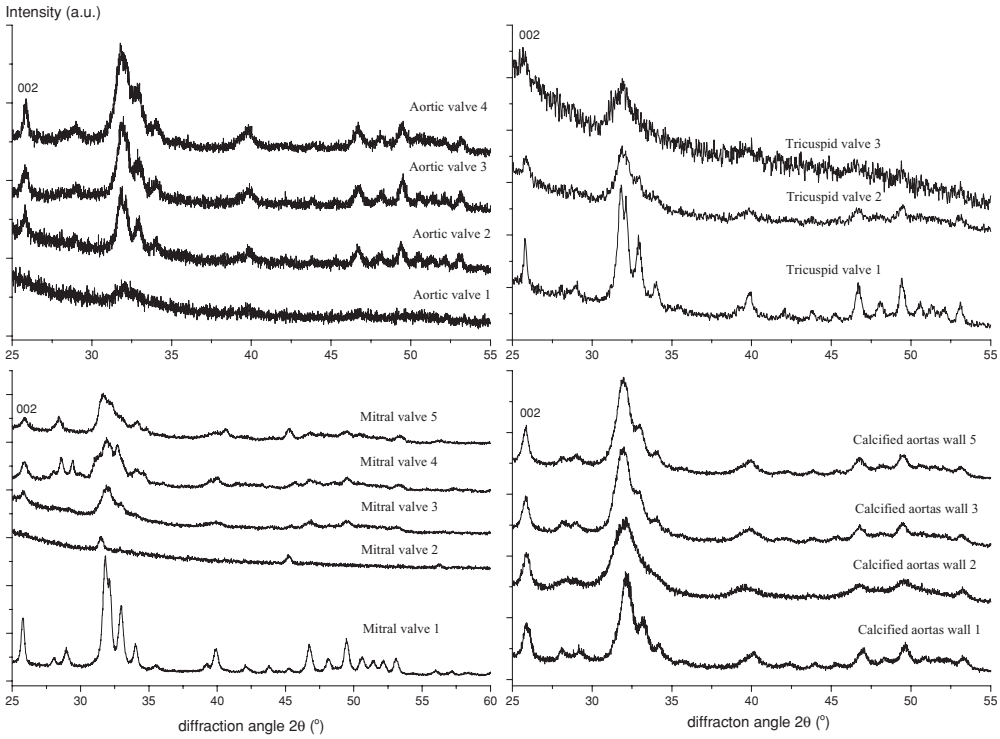

Fig. 3 X-ray diffraction patterns of human cardiovascular deposits at the original state.

the data obtained it was impossible to ascertain, if these additional elements belonged to the apatite lattice or to non-apatite fractions of the biomineral.

The EDX data in all cases (for all kinds of sample and both instruments), gave the Ca to P ratio much higher than the standard value for stoichiometric calcium hydroxyapatite, 1.67 at.%. The determined Ca/P ratios had significant spread in values at local points of the analysis for each sample and varied from 2.04 at.% (Aortic valve 4) to 2.95 at.% (Mitral valve 1).

The X-ray diffraction patterns of the initial and treated at 200 °C samples indicated the presence of nanocrystalline apatite (Fig. 3). As it follows from the diffraction peak broadening, the apatite crystallinity of cardiovascular deposits is mostly very similar to that of bone apatite. However, for some samples (e.g., Tricuspid valve 1 and Mitral valve 1) the degree of apatite crystallinity (average size of apatite crystals) was essentially bigger. The semiquantative evaluation of the crystallite size was carried out by means of physical broadening of the (002) line profile using Scherrer's formula at negligible lattice microstrain in the same way as in the former works [e.g., 10,11]. Powdered polycrystalline NaCl was used as the reference material free of size and microstrain broadening. The crystallite size estimation gave a wide range of values: from 40 nm (Tricuspid valve 1) to

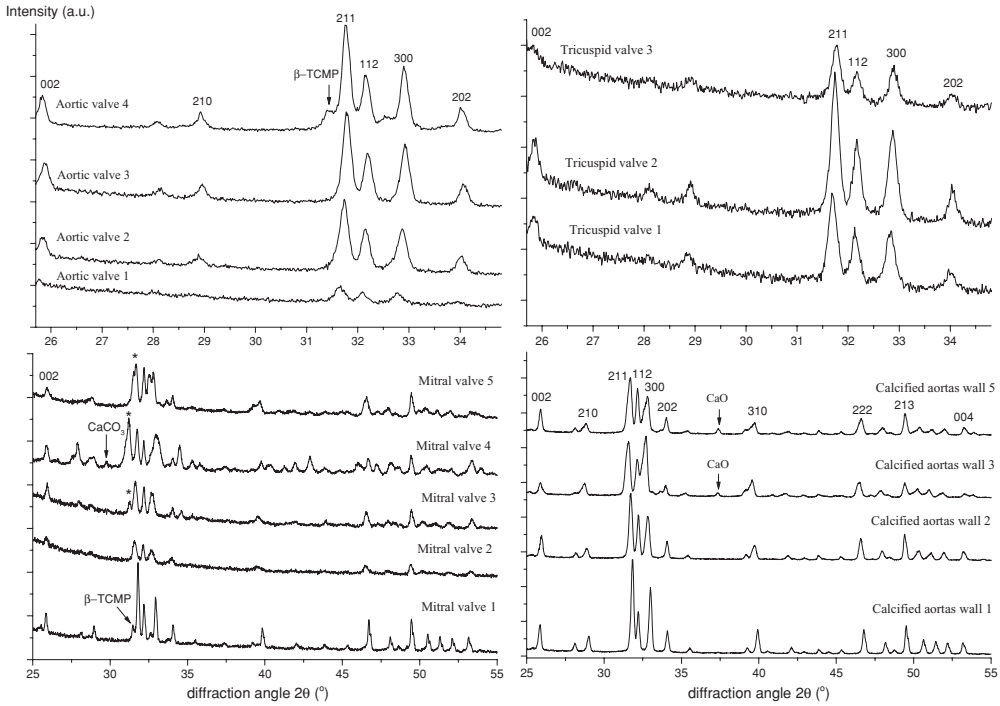

Fig. 4 X-ray diffraction patterns of human cardiovascular deposits annealed at 900 °C. The position of main apatite peaks is marked by the appropriate Miller's indices; the asterisk marks the major peak of β-TCMP.

15.8 nm (Mitral valve 4) and less for the samples where the (002) line was too small and diffused for correct estimation (Aortic valve 1).

Special attention should be paid to the samples Mitral valve 4 and Mitral valve 2. In the first of them, in addition to apatite, the presence of a significant amount of β-TCMP phase and trace amount of $CaCO_3$ was clearly seen. The diffraction pattern of Mitral valve 2 contains only three reflexes which, however, with some tolerance, can be ascribed to (300), (400) and (500) lines of apatite.

It is also essential that for the samples with minimal apatite crystallinity (e.g., Aortic valve 1 and Tricuspid valve 3) the presence of an amorphous component was observed. There was a noticeable tendency of inverse correlation between the intensity of the apatite diffraction lines and the intensity of halo rising while the intensity of the crystal phase lines decreased).

As expected, after the annealing of calcified deposits under the temperature of 900 °C during one hour the recrystallization growth of apatite crystals was observed, accompanied in some cases by the formation of additional crystal phases, the main of which is the β-TCMP phase (figure 4).

Surprisingly, β-TCMP was only found in four of five Mitral valve samples, while it was not found in any of Calcified aorta's walls and Tricuspid valves samples. In small amounts the β-TCMP phase was present only in one of four samples of Aortic valve. The evaluated data of apatite/β-TCMP ratio are listed in table 2. The CaO crystal phase was present in small amount in two samples of Calcified aorta's wall.

It is interesting to note, that the sample Mitral valve 2, initial diffraction pattern of which consisted only of three uncertainly distinguishable lines, after annealing at 900 °C had shown the precise and unequivocal diffraction pattern of apatite.

After careful phase analysis of the pathological calcified deposit samples annealed at 900 °C with the selection of the most suitable phases of apatite family from a database, their additional crystal-chemical features had been revealed. As it appeared, in most cases, the formed apatite phases were not the simple classical hydroxyapatite of calcium, $Ca_{10}(PO_4)_6(OH)_2$ (JCPDS no.9-432), but more complex phases of the apatite family with various isovalent and heterovalent replacements in the anionic and cationic sublattice (table 2). This indicates that the mineral component of calcified deposits contained, additionally to Ca and P, other elements foreign to stoichiometric hydroxyapatite of calcium. The presence of these elements in the bioapatite of pathological

Table 2 XRD characteristics of cardiovascularin deposits in original state and subjected the annealing under the temperature of 900 °C.

Samples		Crystallite size of initial bioapatite from (002) line width, nm	XRD data of biomineral's samples annealed at T = 900 °C	
			Phase content (reference JCPDS data)	Apatite/β-TCMP phase ratio
1	Aortic valve 1	–	Apatite* (82-1943)	
2	Aortic valve 2	30,2	HAp* (89-6438)	
3	Aortic valve 3	23,4	HAp (9-432)	
4	Aortic valve 4	32,1	HAp (89-4405) + β-TKMΦ	81,3 / 18,7
5	Mitral valve 1	33,1	HAp (76-694) + β-TKMΦ	80,2 / 19,8
6	Mitral valve 2	–	Apatite (70-794)	
7	Mitral valve 3	16,0	Apatite (70-794) + TKMΦ (79-2186)	71,1 / 28,9
8	Mitral valve 4	15,8	HAp (9-432) + TKMΦ (77-692) + $CaCO_3$ (5-586)	46,0 / 54,0
9	Mitral valve 5	20,3	Apatite (89-6444) + Apatite (70-795) + $NaCaPO_4$ (29-1193) + TKMΦ (20-348) / (79-2186) + KCl (73-380)	nearly50 / 50
10	Calcified aorta's wall 1	17,8	HAp (89-6437)	
11	Calcified aorta's wall 2	17,3	Apatite (89-6449)	
12	Calcified aorta's wall 3	18,5	Apatite (70-794) + CaO (37-1497)	
13	Calcified aorta's wall 4	–	Apatite	
14	Calcified aorta's wall 5	20,2	Apatite (82-1943) + CaO (77-2376)	
15	Tricuspid valve 1	40,0	Apatite (89-6444)	
16	Tricuspid valve 2	23,6	HAp (89-4405)	
17	Tricuspid valve 3	19,3	HAp (89-4405)	

*"HAp" indicates stoichiometric hydroxylapatite of calcium $Ca_{10}(PO_4)_6(OH)_2$; "Apatite" indicates nonstoichiometric apatites with various substitutions in anionic and cationic sublattice, for example: Apatite (89-6449) is Calcium Sodium Magnesium Phosphate Apatite.

cardiovascular calcifications was also possible, but to verify this experimentally we should exclude the interphase migration of the elements in a high-temperature treatment.

The FTIR spectra of the deposits initial samples showed the characteristic absorbance bands of apatite, though their expanded width is due to low crystallinity of mineral (figure 5). The bands at 1000–1100 cm^{-1} and 500–600 cm^{-1} correspond to different modes of PO_4 group in hydroxyapatite (the phosphate stretching vibrations and phosphate bending vibrations, correspondingly). The bands at 3450 cm^{-1} and 1650 cm^{-1} can be assigned to hydroxyl groups and water present in the structure of mineral and in surrounding material. The bands at 2800–2950 cm^{-1} belong most probably to C-H stretch from the organic components of the deposits.

It should be pointed, that the spectra show the patterns associated with carbonate-substituted apatite. The bands at 1420–1550 cm^{-1} and at 875 cm^{-1} are derived from carbonate ions in apatite structure. Based on literature data [13–15] we suggest that the bands at 872 cm^{-1} and 1418 cm^{-1} are characteristic for B-type carbonate apatite (CO_3^{2-} ions in phospate tetrahedron position).

Therefore, as judged by FTIR data, in all the examined samples the mineral component of cardiovacular deposits was carbonated apatite with significant substitution of phosphate by carbonate ions.

In general, our XRD, EDX and FTIR results had shown that all studied samples consisted of apatite with different crystallinity and variable chemical content, being represented by the formula:

$$(Ca, Na, Mg, X)_{10}(PO_4, HPO_4, CO_3)_6(OH, Y)_2 \quad (1)$$

$$X = K^+, Mn2^+ \text{etc.}$$

$$Y = F^-, Cl^-, CO_3^{2-} \text{ etc.}$$

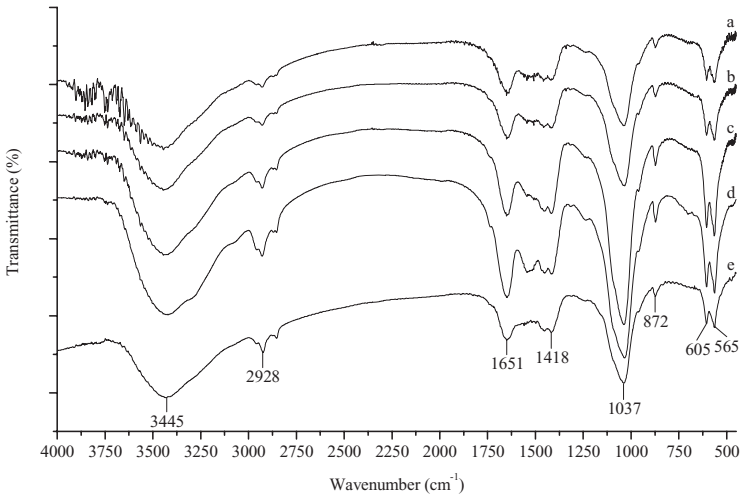

Fig. 5 FTIR spectra of the deposits: a, b, c, d are the spectra from "Aortic valves" placed from up to down with the increasing moiety of B-type carbonated component (at 872 cm^{-1} and 1418 cm^{-1}); e is the spectrum from the sample Tricuspid valve 1.

Therefore, our results are in good agreement with the studies [1,2,4], where formula (1) was introduced as the generalized formula for bioapatite of pathological cardiovascular calcifications (usually the end product of ectopic biomineralization in the cardiovascular system).

The absence of crystalline phases containing Ca and not containing P (e.g., CaO, $CaCO_3$) in both the initial and annealed samples in quantities sufficient to explain the high values of the Ca/P ratio indicates that the excess calcium could be localized on the surface of apatite crystals and/or that the planes forming the outer edge of crystals contained mainly Ca ions. Indeed, the formula (1) proposed by many authors for biological apatite of pathological calcifications, under any possible values of the elements concentrations, does not give the Ca/P ratio close to those measured by EDX. This can be explained by the fact that this formula is valid for an infinite crystalline continuum and does not consider the possibility of crystals being faceted by planes with an excess of Ca and deficiency of P. Of course, in this case, the effect of excess calcium detection will be the more pronounced the larger the surface/volume ratio of such multi-crystal systems is, which is exactly the case for nano-sized crystals of pathological calcifications apatite. Quantitative confirmation of this suggestion requires further experiments and model estimations, which should take into account the surface/volume ratio of hypothetical bioapatite crystals and surface density of excess Ca. In any case, we can say that the boundary surface of apatite component of pathological mineral deposits was characterized by excess Ca content, which was located in the faceting planes of crystals, or in so called non-apatite environment. Combined localization of the excess calcium in both these positions is also possible.

The series of samples called "Aortic valve" was subjected to most complete examination by whole set of instrumental techniques (XRD, IRS, EDX) in order to find qualitative correlations between crystallinity, Ca/P ratio and degree of carbonate substitution in apatite's lattice of the biomineral. As a result, it had been found that the crystallinity and the fraction of the carbonate component grew while the Ca/P ratio decreased in the series Aortic valve 1 $\rightarrow$ Aortic valve 3 $\rightarrow$ Aortic valve 2 $\rightarrow$ Aortic valve 4. This finding supports the idea of direct proportionality between excess of Ca and surface-to-volume ratio in apatite nanocrystals of pathological deposits. Also it is natural that the content of carbonate component was less in less crystallized apatite because $CO_3^{2-} \rightarrow PO_4^{3-}$ substitution requires enough lattice volume.

The important role of biogenic apatite crystal surfaces in the processes of interaction of mineral and organic content in deposits implies the need for a detailed study of the morphology, orientation and size characteristics of the nanocrystals themselves and the state of their surface and the surrounding environment. In accordance to TEM data, the crystals of pathological calcified deposit mostly had oblong or rod-like shape (length 60–90 nm, width 20–30 nm) (figure 6, above). Characteristically, the width of the crystal had a much smaller range of values than the length. At the same time, the spheroid particles of complex ultrastructure had been found (figure 6, below). Electron diffraction patterns confirmed the apatite nature of nanocrystals both rod-like (nanorods), and in the form of complex structures with signs of spherical symmetry, which is consistent with the results of X-ray

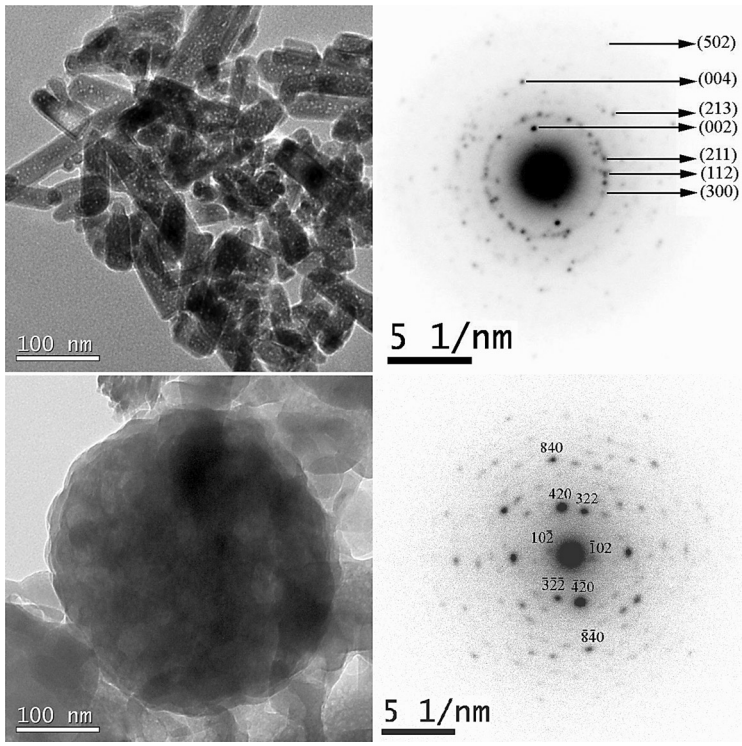

Fig. 6 TEM micrographs and electron diffraction data (JEM2010) for the mineral from human heart valves (above: Mitral valve 1; below: Calcified aorta's wall 4; on the right – the Miller's indices for apatite).

diffraction study of corresponding calcifications at macroscopic scale. Electron diffraction pattern in the case of nanorods was characteristic for polycrystalline material with a small amount of crystals in diffracting position (not continuous diffraction rings are formed by point reflections from single crystals), while the diffraction pattern of a spherical particle was a superposition of the diffraction patterns from several single crystals with visible signs of the spatial order of the individual crystals relative to each other (the location of points on the imaginary rings was regular and orderly).

It should be noted that the preparation of samples for TEM studies included sequential heating (200 °C) and sonication of calcification material in order to remove the organic component and to disperse the crystals of biomineral. Obviously, the particles with spherical geometry were formed from simple-shaped nanocrystals and preserved their complex structure only because of insufficient energy of ultrasonic dispersion (and, perhaps, heat of treatment).

An important addition to the above experimental evidence of specific morphology and complex ultrastructure of pathological deposits' nanocrystals was the SEM data on the existence of planar sheet-like bioapatite crystals (figure 7). Heat pretreatment of the samples at 200 °C and the presence only of Ca and P peaks (with appropriate ratio) in the EDX spectra, strongly suggests that these formations of unusual morphology are mineral and relate to apatite, especially as the X-ray diffraction patterns of the corresponding macroscopic samples confirms this.

Probably, these two-dimensional calcium phosphate formations nucleated and grew on the smooth surfaces of a tissue, and are an example of template-directed growth of crystal structures on organic substrates.

The existence of calcium phosphate crystalline formations with different morphology in pathological deposits suggests different mechanisms of their origin and growth [6,16–18]. The possibility of transformation of one morphological state to another is also cannot be excluded, the more so, that there are many works describing intended and controllable morphological and phase transformations of calcium phosphates in model systems [19–24]. The choice of one or another mechanism of formation and self-assembly of biocrystals by a biological system is probably defined by organic medium and the characteristics of soft tissues at the site of pathological deposition.

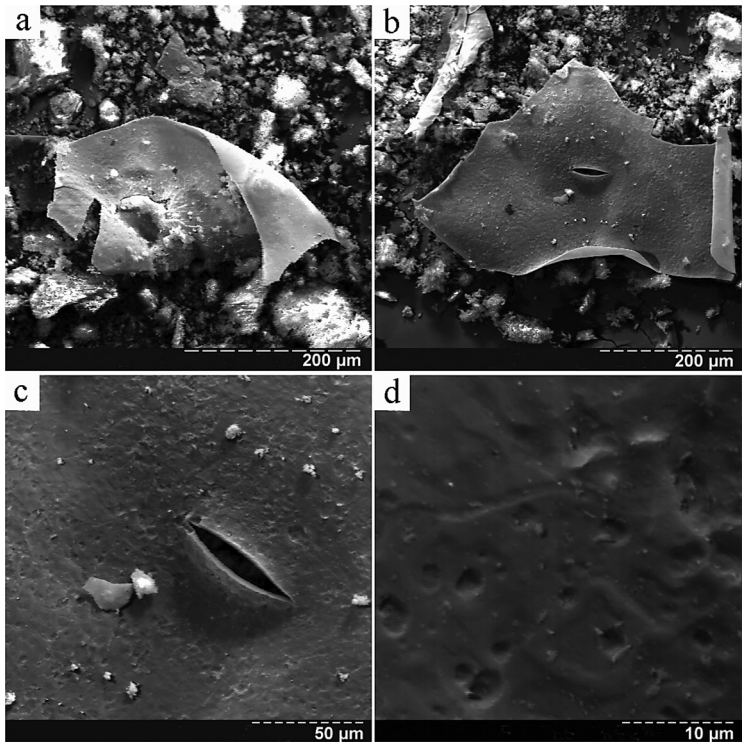

Fig. 7 SEM images (REMMA102) of a deposits' mineralized particle with sheet-like shape (Mitral valve 5 annealed at 200 °C; b, c and d are the same object at the different magnification: 300, 1000 and 5000, respectively).

4 Conclusions

According to the results of the detailed studies using XRD and IRS techniques, all studied samples of cardiovascular calcified deposits in the initial state are poorly crystalline, defective carbonated apatite mainly of B-type (CO_3^{2-} ions substitute group PO_4^{3-}). From the XRD and EDX data, cardiovascular deposit's biomineral can represent either phase-pure calcium hydroxyapatite, or the more complex phases of the apatite family with a variety of isovalent and heterovalent substitutions in the anion and cation sublattices (with the presence of a wide range of foreign elements such as Na, Mg, K, Cl, Fe, S, etc. in their structure). At the level of a trend the dependence of the phase (and chemical) purity of biomineral on the localization of deposit had been observed, for example, β-TCMP was found (in the annealed samples) in four of five Mitral valves and it was not found in any samples of Calcified aorta's walls and Tricuspid valves.

Significant excess of Ca, compared to stoichiometric calcium apatite, was found in the pathological minerals according to EDX analysis, indicating the specific state of the bioapatite nanocrystals surface; the surplus calcium probably being localized on their faceting crystal planes and/or in their non-apatite amorphous environment.

TEM and SEM observations have revealed several forms of nanocrystalline bioapatite with different morphological and ultrastructural characteristics, which is a convincing proof of the existence of several different mechanisms of cardiovascular calcium phosphate deposits' formation and growth. Clarifying these mechanisms will require further special studies of the ultrastructural and crystal-chemical characteristics of each morphological form.

The results of this study could serve as one more evidence that the techniques and methods of sample preparation are really critically important if one wants to obtain complete and undistorted information on the microscopic morphology, orientation, size and ultrastructural characteristics of nanostructured calcified pathological deposits.

Acknowledgments This research was partially supported by the Ukrainian State Agency for science, innovation and informatization (Grant No 0112U003619) and by Chinese Academy of Sciences within the bilateral project "Formation mechanism and structural properties of apatite crystals with specific morphology during pathological mineralization process".

The authors thank Professor D.D. Zerbino, Lvov National Medical University, Institute of clinical pathology, Lvov, Ukraine for the first set of samples (aortic valves and tricuspid valves).

References

[1] R. Z. LeGeros, Zeitschrift für Kardiologie **90** Suppl 3,116 (2001).
[2] B. B. Tomazic, Zeitschrift für Kardiologie **90** Suppl 3, 68 (2001).
[3] M. Epple and P. Lanzer, Zeitschrift für Kardiologie **90** Suppl 3, 2 (2001).
[4] L. G. Gilinskaya, T. N. Grigorieva, G. N. Okuneva, and Yu. A. Vlasov, J. Structural Chemistry **44**, 622 (2003).
[5] L. Stork, P. Müller, R. Dronskowski, and J. R. Ortlepp, Zeitschrift für Kristallographie **220**, 201 (2005).
[6] A. Becker, M. Epple, K. M. Müller, and I. Schmitz, J. Inorganic Biochemistry **98**, 2032 (2004).
[7] D. Mikroulis, D. Mavrilas, J. Kapolos, P. G. Koutsoukos, and C. Lolas, J. Mater. Sci.: Mater. Med. **13**, 885 (2002).
[8] S. E. Etok, E. Valsami-Jones, T. J. Wess, J. C. Hiller, C. A. Maxwell, K. D. Rogers, D. A. C. Manning, M. L. White, E. Lopez-Capel, M. J. Collins, M. Buckley, K. E. H. Penkman, and S. L. Woodgate, J. Mater. Sci. **42**, 9807 (2007).
[9] S. N. Danilchenko, I. Yu. Protsenko, and L. F. Sukhodub, Cryst. Res. Technol. **44**, 553 (2009).
[10] S. N. Danilchenko, A. V. Koropov, I. Yu. Protsenko, B. Sulkio-Cleff, and L. F. Sukhodub, Cryst. Res. Technol. **41**, 263 (2006).
[11] S. N. Danilchenko, O. V. Kalinkevich, M. V. Pogorelov, A. N. Kalinkevich, A. M. Sklyar, T. G. Kalinichenko, V. Y. Ilyashenko, V. V. Starikov, V. I. Bumeyster, V. Z. Sikora, and L. F. Sukhodub, J. Biomed. Mater. Res. Part A **96A**, 639 (2011).
[12] J. I. Goldstein and H. Yakowitz, Practical scanning electron microscopy. Electron and ion microprobe analysis, Plenum Press, New York and London 1975.
[13] J. C. Elliott, Structure and chemistry of the apatites and other calcium orthophosphates, Elsevier, Amsterdam 1994.
[14] M. Markovic, B. O. Fowler, and M. S. Tung, J. Res. Natl. Inst. Stand. Technol. **109**, 553 (2004).
[15] S. Marković, L. Veselinović, M. J. Lukić, L. Karanović, I. Bračko, N. Ignjatović, and D. Uskoković, Biomed. Mater. **6**, 1 (2011).
[16] W. Mohr and E. Görz, Zeitschrift für Kardiologie **92**, 60 (2003).
[17] E. I. Suvorova and P. A. Buffat, Journal of Long-Term Effects of Medical Implants. **15**(4), 355 (2005).
[18] O. L. Katsamenis, V. Karoutsos, K. Kontostanos, E. C. Panagiotopoulos, H. Papadaki, and N. Bouropoulos, Cryst. Res. Technol. **47**, 1201 (2012).
[19] Yanjie Zhang and Jinjun Lu, Nanotechnology **19**, 1 (2008).
[20] Hui Gang Zhang, Qingshan Zhu, and Yong Wang, Chem. Mater. **17**, 5824 (2005).
[21] Kaili Lin, Jiang Chang, Yingjie Zhu, Wei Wu, Guofeng Cheng, Yi Zeng, and Meiling Ruan, Cryst. Growth Des. **9**, 177 (2009).
[22] K. Sandin, L. Kloo, P. Nevsten, R. L. Wallenberg, and L.-F. Olsson, J. Mater. Sci: Mater Med. **20**, 1677 (2009).
[23] Cuimiao Zhang, Jun Yang, Zewei Quan, Piaoping Yang, Chunxia Li, Zhiyao Hou, and Jun Lin, Cryst. Growth Des. **9**, 2725 (2009).
[24] Qian Jun He and Zhi Liang Huang, J. Porous Mater. **16**, 683 (2009).

